THE INFLUENCE OF ORIENTATION, TEMPERATURE AND FREQUENCY ON FATIGUE CRACK GROWTH IN A NICKEL-BASED SUPERALLOY SINGLE CRYSTAL

M.B. Henderson and J.W. Martin

Oxford University Department of Materials
Parks Road, OXFORD OX1 3PH, UK

Abstract

The FCG characteristics of SRR99 have been studied in air at 650°C and 850°C at 10 Hz and 1 Hz with an R ratio of 0.1, using CT specimens with the following crack planes (hkl) and propagation directions [UVW]: (001)[010], (110)[$\bar{1}$10], and (111)[$\bar{1}$10].

At 650°C, the (110) and (111) crack plane specimens showed a frequency-dependent FCG rate, not apparent in the (001)[010] specimens, due to an increased shear stress on the cuboidal cross-slip system giving increased cross-slip at the lower frequency and thereby reducing the reversibility of slip. Homogenization of slip at 850°C prevented this effect.

All specimens showed an improved threshold response at 850°C compared to that at 650°C due to enhanced oxide closure of the crack.

Within the Paris regime, the (001)[010] specimens demonstrated a lower FCG rate at 850°C than at 650°C, due to an increased crack bifurcation at the higher temperature. Conversely, a higher FCG rate with increase in temperature occurs in the (110) and (111) specimens, since the crack path decreases in tortuosity as it changes from propagation along the γ/γ' interface to γ'-precipitate cutting.

The orientation-dependence of FCG rate and fracture path is influenced by the relationship between the crack front and the slip systems available for crack tip shear.

At 650°C, those orientations most able to accommodate crack tip shear on primary slip planes that are near-parallel with the crack front provide the best FCG resistance, whilst at 850°C the best FCG response is found for the same orientations that have now developed large scale ridges as a result of out-of-plane cuboidal slip activity.

Superalloys 1992
Edited by S.D. Antolovich, R.W. Stusrud, R.A. MacKay,
D.L. Anton, T. Khan, R.D. Kissinger, D.L. Klarstrom
The Minerals, Metals & Materials Society, 1992

Introduction

Life prediction calculations for single crystal turbine blades must take into account the possible growth of cracks during the service life, and a material design objective should be to minimize crack growth rates under both creep and fatigue loading conditions. The present work explores the effect of orientation, temperature and frequency upon fatigue crack growth (FCG) in single crystals of SRR99.

Experimental Materials and Methods

The nominal composition of SRR99 (wt %) is as follows: 5.5 Al, 2.2 Ti, 8.5 Cr, 5.0 Co, 2.8 Ta, 9.5 W, 0.015 C, balance Ni.

Cast single crystals of 40 mm diameter and 100 mm length were given a solution-treatment of 4 h at 1300°C followed by a standard ageing-treatment consisting of 1 h at 1100°C then 16 h at 870°C, with interstage air cooling. This procedure resulted in a microstructure consisting of a γ-matrix containing <100>-aligned regular cuboidal arrays of γ' having an edge length of 0.2 to 0.3 μm, occupying approximately 70% of the volume.

Three series of CT-specimens were prepared from the crystals: the orientations of the crack plane (hkl) and of the crack propagation directions [UVW] being respectively (100)[010], (110)[$1\bar{1}0$] and (111)[$1\bar{1}0$]. Figure 1 (a-c) shows diagrammatically the geometry of the machined notch of the CT specimen with respect to the {111} planes available in each case for deformation at the crack tip.

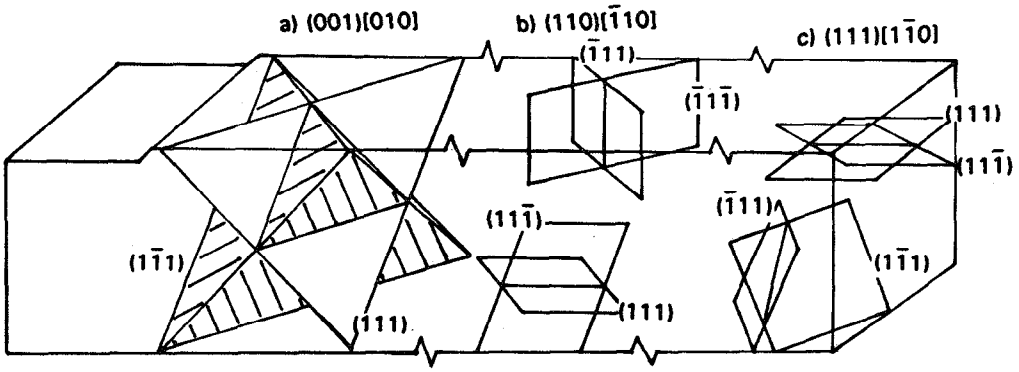

Figure 1. Schematic montage of the arrangement of octahedral planes with respect to the CT specimen machined notch front for a) (001)[010], b) (110)[$1\bar{1}0$] and c) (111)[$1\bar{1}0$] orientations.

Fatigue crack growth (FCG) tests have been conducted under constant load amplitude in air at 650°C and 850°C according to ASTM E647-86a. A triangular waveform was utilised and the crack length monitored using a DC potential drop technique. The FCG rates have been compared at test frequencies of 10 Hz and 1 Hz, and da/dN vs ΔK curves have been established for R=0.1. A number of interrupted tests were conducted in which the fatigue cracks were grown to a ΔK level within the Paris regime and the specimen was then removed from the load frame and sectioned longitudinally, and the crack path examined by SEM. Fractographic examination of the test specimens was also carried out. In all of the micrographs shown, the FCG direction is from left to right.

Experimental Results

(001)[010] crack plane specimens.

Figure 2 shows the da/Dn vs ΔK FCG curves obtained at 850°C and 650°C at 10 Hz and 1 Hz. It is seen that at the lower frequency there is an improved near-threshold response, suggesting an enhanced oxidation of the fracture surface leading to closure reducing the effective ΔK. Throughout the Paris regime the FCG rate at the lower temperature is greater than at 850°C.

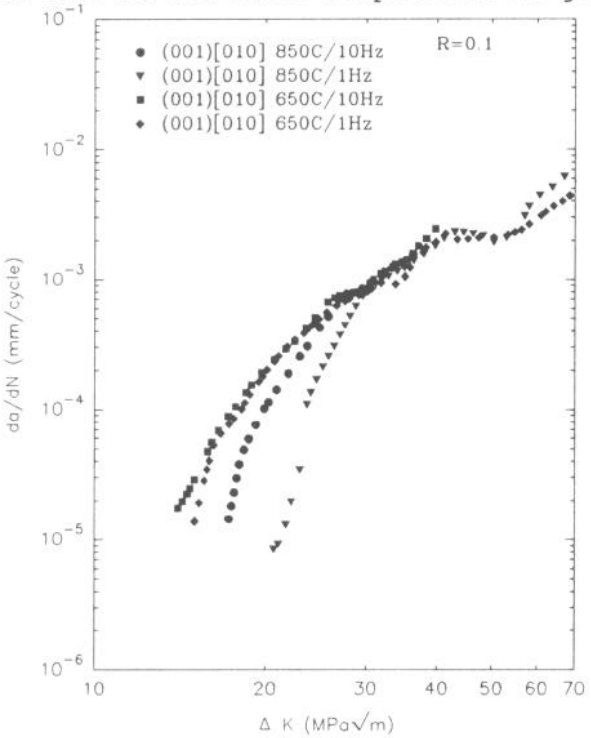

Figure 2. FCG curves for standard aged SRR99 (001)[010] oriented specimens.

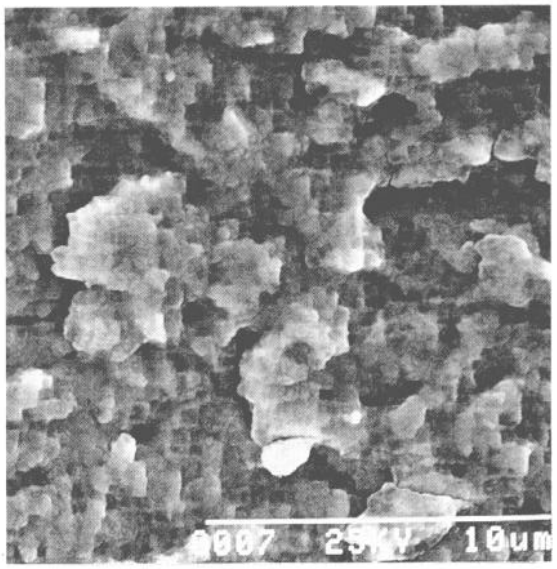

Figure 3. (001)[010] 650°C 10 Hz fatigue fracture face. ΔK=18MPa√m. SEM micrograph.

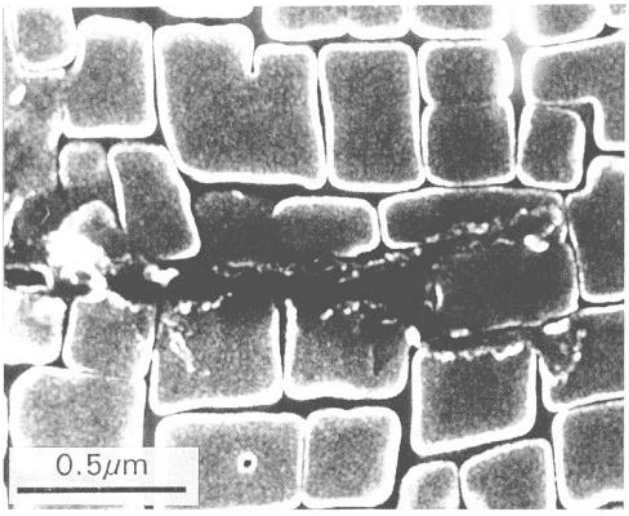

Figure 4. (001)[010] 650°C 10 Hz Stage II fatigue crack in standard aged SRR99. ΔK=23MPa√m.

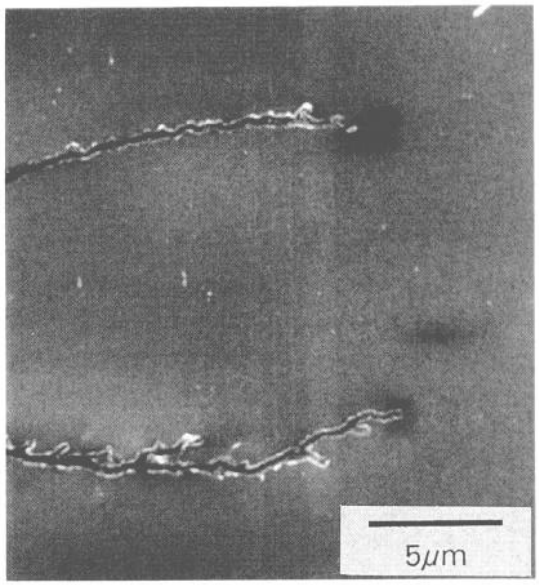

Figure 5. (001)[010] 850°C 10 Hz Stage II bifurcated fatigue crack in SRR99. ΔK=25MPa√m. SEM micrograph.

At 650°C crack propagation is predominantly Stage II on the (001) plane. Figure 3 shows the fracture face, just ahead of the precrack, in which precipitate cutting is indicated by differential oxidation of the matrix and γ'. The fracture face is seen to be predominantly flat. A sectioned crack taken from a test interrupted at a high ΔK in the mid-Paris regime is shown in the SEM image of Figure 4. This confirms the planar nature of the fracture path and the crack at this ΔK level is contained mainly within the matrix and at the γ/γ' interface, although some precipitate cutting is occurring. The tip of the crack is seen to be bifurcated as it propagates around an obstructing precipitate and close examination revealed fine scale intense shear bands cutting the γ'.

At 850°C stage II propagation again dominates, the crack path is confined mostly to the matrix throughout the ΔK range employed, and is heavily oxidised. Figure 5 shows a large bifurcated crack which meanders locally as it bypasses individual γ' particles, but is macroscopically flat and featureless when examined fractographically.

Specimen failure at high ΔK levels is associated with a transition from stage II to stage I-type propagation along the (111) and (1$\bar{1}$1) planes leading to large, isolated octahedral facets. This occurs at about the same ΔK level for all the testing conditions corresponding to the change in gradient at high ΔKs seen in Figure 2.

(110)[1$\bar{1}$0] crack plane specimens.

Figure 6 shows the FCG curves for this orientation. The 850°C curves are seen to cross the 650°C curves at a low ΔK level for these specimens. At 650°C, in contrast to the (001)[010] specimens, the 10 Hz FCG rate is reduced in comparison with that at 1 Hz for most of the Paris regime. At 850°C the 1 Hz data exhibit a higher near-threshold response than the 10 Hz data, but the curves converge during the Paris regime and fail at the same ΔK level, but at a lower level than that observed at 650°C. No stage II to stage I transition was observed, and the high ΔK region of the 850°C fracture face, when viewed by SEM, displayed a large areal fraction of interdendritic porosity compared with that seen at 650°C.

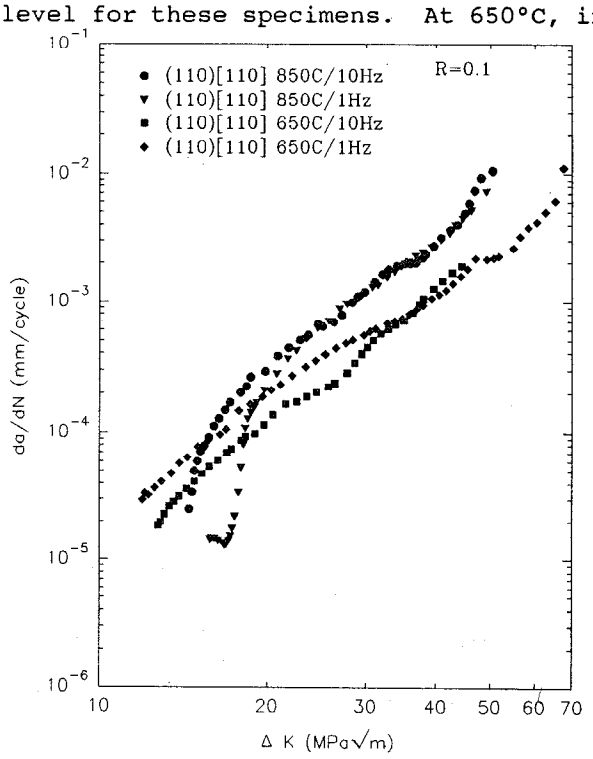

Figure 6. FCG curves for standard aged SRR99 (110)[1$\bar{1}$0] oriented specimens.

SEM examination of the path of a sectioned crack showed that at 650°C at low ΔKs the precipitates were being cut by the crack and a gradual transition occurred from γ' cutting along (110) to avoidance of the particles by the crack as ΔK increases. Figure 7 illustrates propagation mainly along the γ/γ' interface. At 850°C the crack shows little evidence of meandering (Figure 8), and some precipitate cutting is taking place. At both temperatures, fractographic evidence showed the fracture faces to be flat, with little evidence of ridge development.

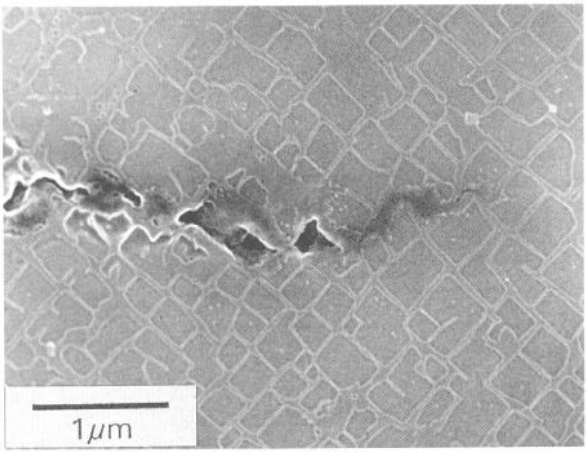

Figure 7. (110)[$\bar{1}$10] 650°C 10 Hz stage II fatigue crack. ΔK=23MPa√m. SEM micrograph.

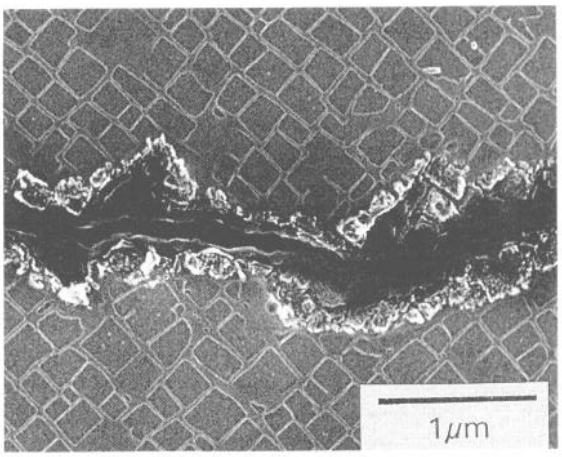

Figure 8. (110)[$\bar{1}$10] 850°C 10 Hz stage II fatigue crack path. ΔK=21MPa√m, SEM micrograph.

(111)[$\bar{1}$10] crack plane specimens.

The FCG curves, shown in Figure 9, reveal a pattern of behaviour similar to that seen for the (110) specimens. The 650°C curves show an increase in FCG rate with reducing frequency, the curves converging at high ΔKs. At 850°C 10 Hz, a sharp threshold response is observed, and in the Paris regime a higher FCG rate is obtained than at 650°C. The 1 Hz curve at this temperature shows a double inflection in the near-threshold regime.

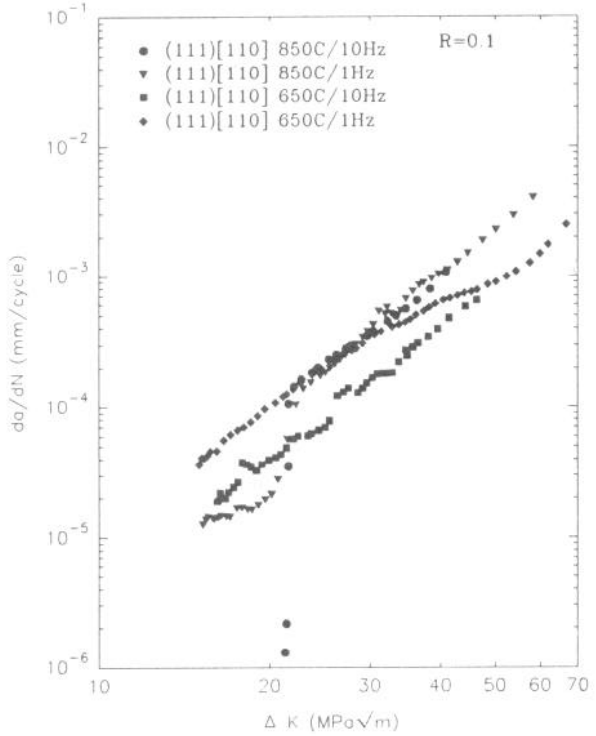

Figure 9. FCG curves for standard aged SRR99 (111)[$\bar{1}$10] oriented specimens.

Within the Paris regime the overall appearance of a sectioned crack at 650°C was found to be similar to that shown in Figure 7, i.e. crack deflection occurs as the crack avoids cutting the γ' by propagating along the γ/γ' interface and within the matrix. SEM fractography of the 650°C fracture faces showed, in the low ΔK regime, predominant stage II propagation along the (111) plane (as evidenced by the triangular shape of the differential oxidation pattern) and a tendency to form macroscopic ridges, as illustrated in Figure 10. The ridges were identified as {100} surfaces from the appearance of the differentially oxidized γ' particles. The ridge features disappeared as ΔK increased and the crack path became confined increasingly to the matrix.

At 850°C the crack path is straight (as seen in Figure 11), with cutting of the γ', and the level of oxidation is high, as is the width of the crack. SEM fractography showed an increased tendency to form extensive ridges parallel to the FCG direction as seen in Figure 12. As seen in Figure 13, definite cuboidal facets were

identified (marked F) at high ΔKs, with striations parallel to {100}. This indicates that the crack front is advancing along these planes by mode II (shear) processes.

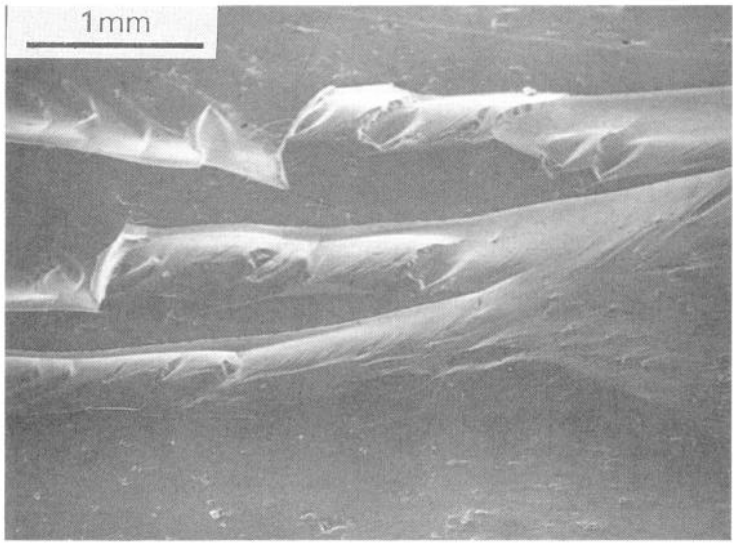

Figure 10. (111)[1$\bar{1}$0] 650°C 10 Hz fracture face. Perspective view of low ΔK region. SEM micrograph.

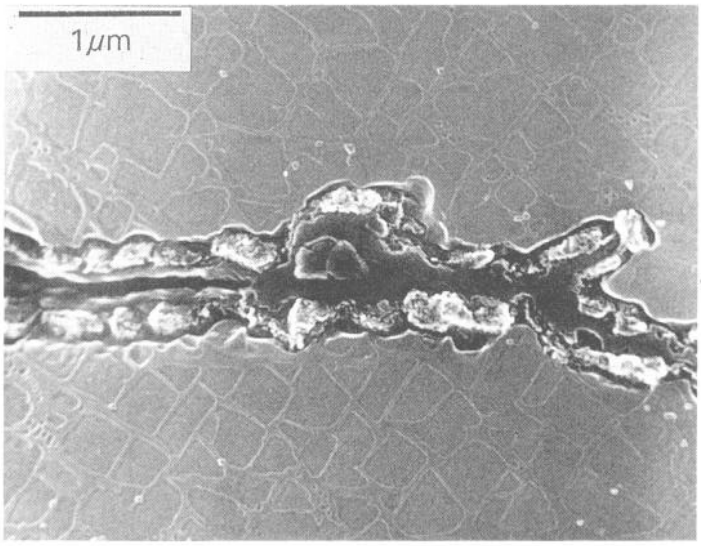

Figure 11. (111)[1$\bar{1}$0] 850°C 10 Hz crack path. ΔK=24MPa$\sqrt{m}$. SEM micrograph.

Discussion

(001)[010] crack plane specimens.

It is clear from Figure 1(a) that there are a number of symmetrically disposed slip planes coplanar with the crack tip. The overall appearance of the fatigue fractures shows that propagation is predominantly via stage II crack extension along the plane of maximum tensile stress normal to the loading axis.

650°C Results. There is little effect on FCG rate as the frequency is reduced from 10 Hz to 1 Hz. The propagation path changes from one of precipitate cutting on (001) to propagation through the matrix and the γ/γ' interface as ΔK increases. Murphy (1) has shown that the crack tip plastic zone size for

SRR99 at 650°C under plane strain conditions is not influenced by a change in frequency from 10 Hz to 0.1 Hz, so no frequency effect on FCG rate is to be expected. Furthermore, the interrupted crack path evidence also shows negligible oxidation of the crack within the Paris regime and this indicates

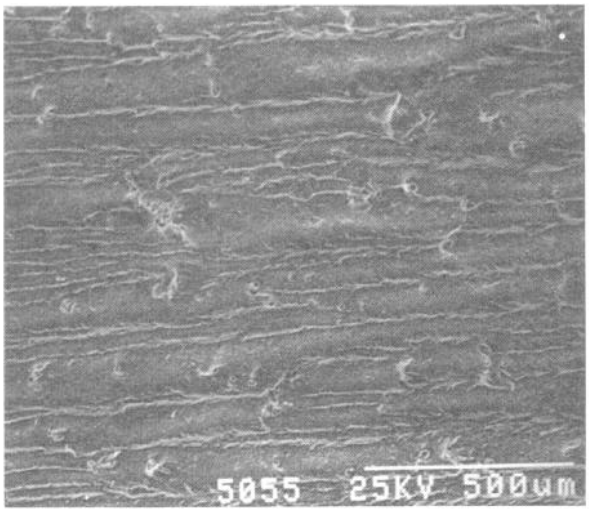

Figure 12. (111)[$1\bar{1}0$] 850°C 10 Hz fatigue fracture face. ΔK=28MPa$\sqrt{m}$. SEM micrograph.

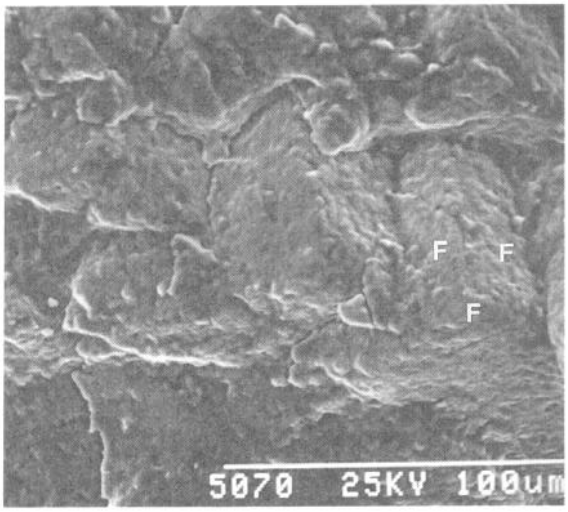

Figure 13. (111)[$1\bar{1}0$] 850°C 10 Hz fatigue fracture face. ΔK=38MPa$\sqrt{m}$. SEM micrograph.

that there is unlikely to be a detectable environmental enhancement of crack growth at this temperature.

850°C Results. The improved thresholds evident in Figure 2 can be accounted for in terms of enhanced oxidation closure giving crack tip-shielding. This is not followed, however, by the expected enhancement of FCG rate within the Paris regime as is often seen (e.g. 2) and is commonly attributed to oxygen embrittlement of the crack tip. Crack meandering is likely to result when there is a combination of enhanced oxidation and a heavily deformed matrix through which the crack tip is forced to extend (3), particularly when the level of dislocation activity within the particles will be limited due to the low resolved shear stress on cuboidal systems. It is clearly shown in Figure 5 that crack tip bifurcation has occurred, and a series of crack branches is apparent along the length of the crack which will have the effect of reducing the crack driving force to such an extent that the 850°C curves do not cross those obtained at 650°C. The curves do converge, however, but the stage II propagation mechanism breaks down and stage I propagation on {111} takes over. The transition to Stage I can be explained in terms of a dislocation recovery model due to Leverant and Gell(4) in which stage I propagation occurs when the FCG rate exceeds the rate of dislocation recovery out of an intense slip band ahead of the crack. This will be favoured by tests at low temperatures and higher frequencies.

(110)[$1\bar{1}0$] crack plane specimens.

Figure 1(b) illustrates that there are no octahedral systems co-planar with the crack tip, and {111} traces will be either parallel with or perpendicular to the crack.

650°C Results. In contrast to the (001)[010] specimens, an increase in FCG rate is observed on reducing the frequency from 10 Hz to 1 Hz. This observation can be rationalised in terms of N, the ratio of the Schmidt factors on the cube cross-slip (010)[$\bar{1}01$] and the primary octahedral (111)[$\bar{1}01$] systems, which is a measure of the shear stress for cube cross-slip. (001)[010] specimens will have identical Schmidt factors on each stress axis and N is essentially zero. The higher value for N for (110) and (111) crack

planes imposes a cross-slip dependency on the FCG response of the material. At a lower frequency more time is allowed for cross-slip of screw dislocations on the activated octahedral systems. This enhances dislocation locking mechanisms which in turn limits slip reversibility and therefore increases the FCG rate at 1 Hz in comparison with that at 10 Hz. A transition in propagation path is seen as ΔK increases from precipitate cutting on (110) to propagation through the matrix, however, due to the orientation of the γ' with respect to the crack front, a bifurcated crack results.

850°C Results. There is no difference observed in the FCG rates when the test frequency is reduced from 10 Hz to 1 Hz at this temperature. Due to thermally activated cross-slip at this temperature, plastic flow is homogenised, and this effect, together with a lower CRSS for cuboidal slip will reduce the strain-rate sensitivity for slip reversibility. The propagation path shows that there is a greater propensity for precipitate cutting as a result of an increase in dislocation activity within the particles, and therefore the level of crack meandering is reduced compared to that seen for (001)[010]. The FCG rate therefore increases with respect to that seen at 650°C, and the curves are seen to cross. The increase in threshold ΔK can be explained in terms of oxide closure.

The difference in ΔK at fracture between tests at 650°C and 850°C can be accounted for by the enhanced crack propagation at interdendritic micropores at high ΔK levels. This ΔK regime is effectively not seen for the (001)[010] specimens due to the stage II to stage I transition.

$(111)[1\bar{1}0]$ crack plane specimens.

Figures 1(c) shows that a number of co-planar octahedral planes are available at the crack tip for deformation at lower temperatures, whilst at 850°C the primary slip system is expected to be cuboidal (also coplanar with the crack tip), the secondary slip being octahedral.

The pattern of behaviour is similar to that observed for the (110) specimens in several regards. Firstly, the increasing FCG rate with reducing frequency can be accounted for on the same basis, namely the increased probability of cuboidal cross-slip reducing the reversibility of slip. Secondly, a lower FCG rate is found throughout the Paris regime on decreasing the temperature. This is again seen to be associated with increased crack path tortuosity at 650°C as the crack path was confined to the γ/γ' interface within the Paris regime.

The 650°C 10 Hz specimens showed large ridges on the fracture surface. It is proposed that they form as a result of cross-slip activity between {111} and {100} planes as a result of the orientation of the crack front with respect to the available slip systems. The ridges are not as prevalent at 1 Hz, although microscopic ridges do develop at moderate ΔK levels. Large scale ridges are evident at both frequencies at 850°C; these will arise from primary cube slip activation on (100) and (010) in the [011] and [101] directions respectively ahead of the crack. These two systems are both at an angle to the crack front and are asymmetrical on either side of the crack plane and therefore ridge formation as proposed by Neumann (5) is to be expected. In addition cuboidal slip can be expected on (001), generating facets that are analogous to the octahedral facets commonly observed on cracks formed at ambient temperature.

The influence of orientation. Comparison of the FCG curves in the Paris regimes show that (110)[110] exhibits the fastest FCG rate, and $(111)[1\bar{1}0]$ the lowest. In terms of the plastic processes at the crack tip, low growth rates will be associated with strain reversibility over the fatigue cycle. Such reversibility would be expected, with the formation of plane fracture surfaces, if the primary slip systems intersect the crack tip (6,7). If the crack tip deformation involves substantial cross-slip, then strain reversibility will be lost and FCG rates enhanced.

In the light of this approach, it can be seen from Figure 1b that the (110)[$\bar{1}$10] specimen is an unsuitable orientation for the accommodation of crack tip plastic shear, as none of the octahedral planes intersect along the crack front. Crack tip deformation must be accommodated by localized shearing and/or tearing and extensive ridge formation should be apparent for this orientation as has been observed previously in austenitic stainless steels (8). The absence of surface ridges implies that the crack tip shear has been accommodated by operation of the (100) cross-slip plane, which intersects the crack front.

Figure 1c likewise indicates that the (111) specimens, though non-symmetrical about the crack plane, are suitably oriented for cube and octahedral slip such that shear accommodation is achieved by primary and secondary slip - which will produce the planar fracture surfaces observed at 650°C. Limited cross-slip activity permits strain reversibility and thus a low FCG rate is achieved. At 850°C the primary slip system will be cuboidal and this leads to out-of-plane slip at the crack tip such that large scale ridges form parallel with the FCG direction.

The orientation-dependence of FCG rate and fracture path is thus influenced by the relationship between the crack front and the slip systems available for crack tip shear. Orientations not containing slip directions normal to the crack front and/or slip planes that pass through the crack front do not necessarily form ridges, due to shear accommodation on cuboidal cross-slip systems.

At 650°C, those orientations most able to accommodate crack tip shear on primary slip planes that are near-parallel with the crack front provide the best FCG resistance, whilst at 850°C the best FCG response is found for the same orientations that have now developed large scale ridges as a result of out-of-plane cuboidal slip activity.

Conclusions

1. At 650°C, (110) and (111) crack plane specimens showed a frequency-dependent FCG rate, due to an increased shear stress on the cuboidal cross-slip system giving increased cross-slip at lower frequency and thereby reducing the reversibility of slip. No such effect was found for (001)[010] due to an essentially zero resolved shear stress for cuboidal activity.

2. All orientations showed an improved threshold response at 850°C compared to that at 650°C due to enhanced oxide closure of the crack.

3. For (001)[010] a lower Paris regime FCG rate was found with increasing temperature from 650°C to 850°C as a result of an essentially planar stage II propagation path at 650°C and a much more bifurcated crack at 850°C.

4. A higher FCG rate in the Paris regime with increase in temperature occurs in the (110) and (111) specimens, since the crack path decreases in tortuosity with increasing temperature as it changes from one of propagation through the matrix and along the γ/γ' interface to one of γ'-precipitate cutting.

5. An orientation-dependence of the FCG rate has been observed and can be accounted for in terms of the crack tip deformation characteristics of the various specimen orientations.

6. Interdendritic microporosity has been found to influence the high ΔK response at 850°C for (111) and (110) orientations, but not for (001) due to the intervention of a stage II to stage I-type propagation.

Acknowledgements

The authors are grateful to the SERC and to the Procurement Executive of the

Ministry of Defence for support, and to Professor Sir P.B. Hirsch, FRS, for the laboratory facilities made available.

References

1. O.R. Murphy, "Fatigue crack propagation in single crystal superalloys" (M.Sc. Thesis, Oxford University, 1987).

2. J.E. King and P.J. Cotterill, "Roles of oxides in fatigue crack propagation "Materials Science and Technology 6 (1990) 19-31.

3. E. Aghion, M. Bamberger and A. Berkovits, "High-temperature low-cycle fatigue of a nickel-based MAR-M200 + Hf alloy in Ar and Ar + 20% O_2 environment" Journal of Materials Science 26 (1991) 1873-1881.

4. G.R. Leverant and M. Gell " The influence of temperature and cyclic frequency on the fatigue fracture of cube oriented nickel-base superalloy single crystals" Met.Trans.A 6A (1975) 367-.

5. P. Neumann, "New experiments concerning the slip processes at propagating fatigue cracks" Acta Metallurgica 22 (1974) 1155-1178.

6. P. Neumann, "The formation and propagation of cracks by cyclic stresses" Z.f. Metallk. 58 (1967) 780-789.

7. R.M.N. Pelloux, "Mechanisms of formation of ductile fatigue striations" Trans. A.S.M. 62 (1969) 281-285.

8. P. Rieux, J. Driver and J. Rieu, "Fatigue crack propagation in austenitic and ferritic stainless steel single crystals" Acta Metallurgica 27 (1979) 145-153.